

Experimental Research and FE Model of a Bolted Steel-CLT Composite Connection

Miloš Milić^{1*}, Todor Vacev¹, Predrag Petronijević¹, Ivan Nešović¹, Andrija Zorić¹, Stepa Paunović², Biljana Matejević Nikolić¹

¹ Department of Civil Engineering, Faculty of Civil Engineering and Architecture, University of Niš, Aleksandra Medvedeva 14, Niš, Serbia

² Mathematical Institute of the Serbian Academy of Sciences and Arts, Kneza Mihaila 36, Belgrade, Serbia

* Corresponding author, e-mail: milos.milic@gaf.ni.ac.rs

Received: 09 June 2023, Accepted: 18 July 2023, Published online: 16 August 2023

Abstract

Steel-timber composite structures have numerous advantages compared to steel only and timber only structures. One of the most important parts of a composite structure is the composite connection. Object of this research was a steel-CLT composite connection consisting of a steel profile, a cross-laminated timber (CLT) panel and a bolt with nut and washer. Aim of the research was to develop an efficient finite element (FE) model of a bolted steel-CLT composite connection and to validate it experimentally. The research process consisted of several steps: experimental testing of the considered connection using asymmetrical push-out test, numerical modelling and analysis of the connection using Finite Element Method (FEM), validation of the numerical model using experimental results, and parametric study of the proposed numerical model. For numerical analysis, an innovative method for timber modelling has been proposed. The comparison between the experimental and numerical research results demonstrated that the proposed numerical model was convenient for practical application in structure analyses. The parametric study showed that, in some cases, atypical failure modes of the connection occurred. Based on registered behavior, a recommendation is given to calculate the load capacity of the connection integrally, taking into account both the primary (Johansen's) and the secondary (rope effect) part of the connection strength, instead partially, as proposed by EN standards.

Keywords

bolted composite connections, steel profile, CLT, push-out test, FE analysis

1 Introduction

In composite structures, the connections that enable composite action is of ultimate importance. Connections for composite action of steel and timber material are very complex for numerical modelling because of the nonlinear material behavior of the consisting parts, and the contact phenomena that are unavoidably present during transfer of forces from one part to another.

A special issue represents the material model for timber that should be able to represent material nonlinearity and orthotropy. Timber can be modelled using continuum, discrete, and hybrid models. The continuum approach to timber modelling is the simplest one from the aspect of model geometry, because it uses volume elements. One of the approaches in continuum modelling of timber is application of the so-called timber foundation model, where the bilinear elastoplastic material model is applied in the zones

where such behavior is expected (around the bolthole) [1]. A more accurate, but also more complex model was developed by Sandhaas [2], who applied the continuum damage model with Tsai-Wu material yield condition. This model can be applied on all orthotropic fibrous materials, and it gave results that coincide very well with experiments, so it has large application in analyses of the dowel-type timber connections [3–5]. Akter et al. [6] apply Hill, Hoffman, and novel Quadratic multi-surface (QMS) failure criterion for defining yield conditions in triaxial anisotropic materials. Based on comparison with experimental results, they conclude that in modelling of the triaxial anisotropic materials, the Hill criterion is insufficiently accurate, and that the novel QMS model is the most accurate. 2D and 3D modelling of timber beams was applied by Saad and Lengyel [7]. Their research is based on the analysis of an elastic and

plastic orthotropic material (biaxial anisotropic), and the conclusion is that Hill’s criterion can be applied for modelling of those materials. The same authors show that material model can be successfully used for modelling of timber with discontinuities – knots [8]. The main disadvantage of the continuum models is the lack of material models that are ready to use in contemporary engineering software. Instead, the user is directed to define the behavior of timber using program subroutines created on its own, which involves thorough knowledge of fracture mechanics.

Avoiding of the continuum modelling, and simplification of the modelling process has been attempted using discrete models, with good results. Discrete models basically imitate the cell structure of timber by lattice structure of finite elements, and certain macroscopic behavior is achieved by defining the parameters of the 1D elements that build the structure of the model. Orthotropic behavior of the material is achieved by element setting in the lattice structure, which may be hexagonal [9] or quadric [10]. One of the 2D discrete models is applied for analysis of the dowel-type timber connections, and in which the influence of the timber is replaced by 2-node ROD elements [11]. However, if very precise results are needed, such models require very dense FE mesh, resulting with high number of FE and long duration of analysis.

Hybrid models are a combination of continuum and discrete models, consisting of volume (3D), surface (2D) and line (1D) FE, and thus keeping their own advantages and disadvantages. Orthotropy is achieved here like in the discrete models, by the appropriate orientation of elements, and material models are taken from the material libraries embedded in various software. In the paper of Racher and Bocquet [12], a combination of elastoplastic line and surface elements is applied, where the line elements are oriented in direction parallel to the timber grain. In the research of Toussaint [13], volume and line elements are used, whereat for the volume elements the foam material model was applied, and for the line elements elastoplastic-bilinear material model. Tavakoli-Gheynani [14] was applied a combination of volume and surface elements, with elastic-orthotropic material model for volume elements, and elastoplastic for surface elements.

Subject of this research is behavior of steel-CLT composite connection, realized by single bolt acting as a shear connector. The main goal was to develop an innovative numerical model of the connection and to validate it by experiments. The proposed numerical model should include all phenomena that affect the mechanical behavior of such

connection, and at the same time to be simple enough for practical application. The proposed model should serve as alteration or replacement for costly and demanding experiments. The model will be subdued to a parametric study with varying of several parameters of the connection in order to reveal their influence on connection strength and stiffness. The varied parameters will include bolt grade, pretension force, and thickness of the steel profile web.

In this research, for timber modelling a hybrid model consisting of combination of line and surface FE has been proposed. It was verified by checking the mesh sensitivity, and validated experimentally, through defined load-slip curves, obtained by push-out tests. The experimental part of the research considered different types of push-out tests, and the asymmetrical type has been selected as the most acceptable.

2 Experimental research

Examination of the mechanical characteristics of shear connectors may be done using the standard symmetrical or asymmetrical push-out test. The symmetrical test (Fig. 1(a)) is more often applied for examination of different connection types because of its simplicity [15–20]. However, a significant drawback of this type of test is existing of two slipping planes between the parts that form a composite structure, so the number of connectors included in the test must be even.

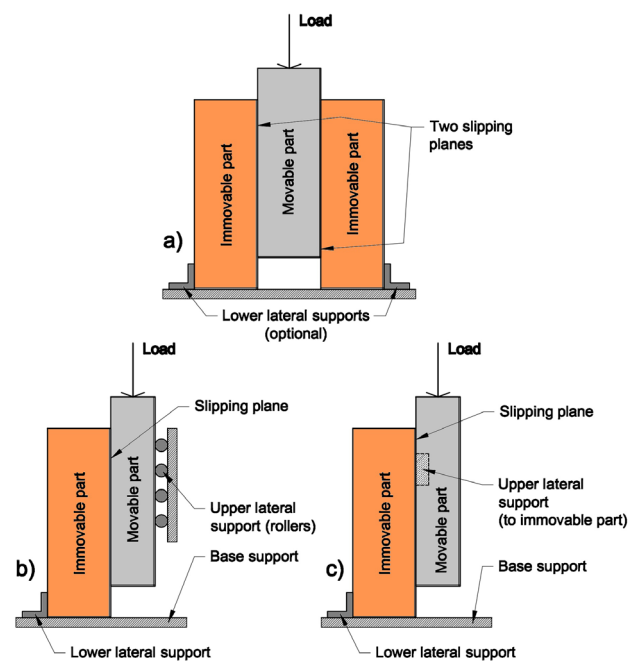


Fig. 1 Types of push-out test: (a) symmetrical, (b) asymmetrical with lateral support of the movable part, (c) asymmetrical with lateral support of the immovable part

Considerably lower number of tests of different connections has been conducted using asymmetrical (pure shear) push-out test. Its advantage is existence of only one slipping plane. A drawback here is potential instability of the examined specimen resulting in overturning, because of the eccentricity of test load action. This requires introduction of lateral support, either for the movable [21–26], or for the immovable [27, 28] part of the specimen. Although in case of the symmetrical test friction between the immovable parts and the base support provides considerable stability during the test, occurrence of the lateral force in the slipping plane is not excluded, so in some research lateral supports nevertheless may be found [29].

In asymmetrical test, if the movable part of the specimen is laterally supported, the lateral supports have form of rollers that enable vertical and prevent horizontal movement of the specimen (Fig. 1(b)). In this case, load applied on the specimen generates additional pressure in the slipping plane. This pressure produces a friction force that may increase the connection strength up to 10% [23]. The variant of the asymmetric push-out test with lateral support placed on the immovable part of the specimen is more favorable regarding stresses, because lateral force does not generate additional pressure in the slipping plane. Besides, this variant has simpler construction, because fixed supports are used instead of roller supports, (Fig. 1(c)). Considering the previous, in this research the variant with lateral support of the immovable part of the specimen has been applied. The specimen consisted of a CLT panel, a steel profile, and one connecting bolt (Fig. 2). The CLT panel was made according to the standard [30], using the botanical timber species Norway Spruce (lat. *Picea Abies*), with class C24 [31]. The CLT panel consisted of five layers 20 mm thick, joined by polyurethane glue, with total dimensions $300 \times 300 \times 100$ mm. The average measured moisture in the panels was 9%, and mass density 460 kg/m^3 .

For the purpose of bolted connection, a hole with diameter of $\text{Ø}10$ mm has been drilled in the middle of the CLT panel. The steel part of the structure consisted of a cold-formed channel profile $\text{U}80 \times 40 \times 4$ mm, with grade S275. Appropriate hole $\text{Ø}10$ mm for bolt connection has been drilled in the steel profile, too, and on the top part of the profile a steel plate 10 mm thick has been welded, for uniform load applying. During the test, the movable part (steel profile) could slide down through a void provided in the base of the testing device.

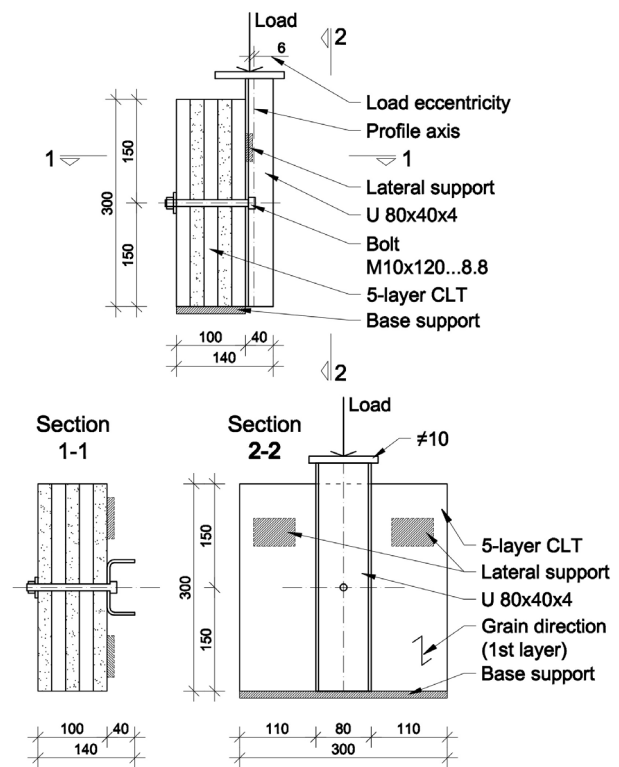


Fig. 2 Details of the push-out test specimen with supports (measures in mm)

As a shear connector, a bolt $\text{M}10 \times 120$ with grade 8.8 has been used. Joining operation was performed immediately before testing, without pretension. The thread part of the bolt was set out from the slipping plane, so the bolt shear occurred only over the gross cross section of the bolt shaft. The CLT panel was oriented such that the load direction was parallel to the grain in the first layer (the nearest to the steel profile). The complete setup of the experiment is presented in Fig. 2.

The testing procedure has been conducted according to the standard EN 26891 [32]. The standard procedure prescribes loading of the specimen up to 40% of the estimated strength (F_{est}), keeping that load for 30 s. Next, the load is reduced to 10% of F_{est} , also keeping it for 30 s (Fig. 3, left diagram). Finally, the specimen is loaded up to the occurring of slipping in the connection measuring 15 mm (Fig. 3, right diagram). The load registered at this slipping value is declared as connection strength, F_{max} . This procedure has been conducted in this research for five specimens. Fig. 4 illustrates the experiment setup with instrumentation for load and slip measuring.

All the materials of the specimens (timber, steel profile, and the bolt) have been examined experimentally, and the input characteristics for the numerical model have been

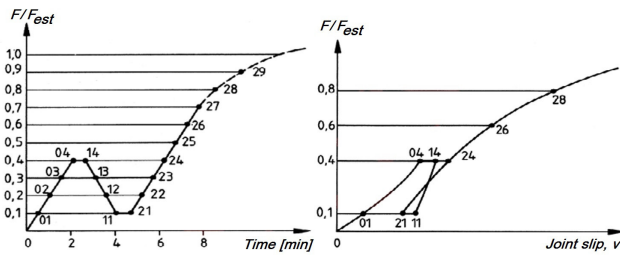


Fig. 3 Loading procedure for push-out test [32]

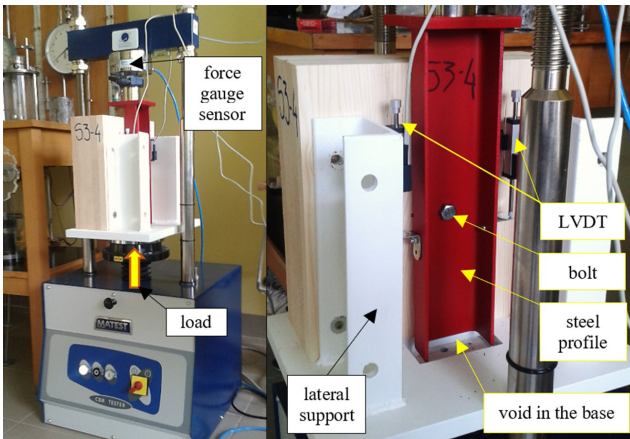


Fig. 4 Push-out specimen with measuring instrumentation

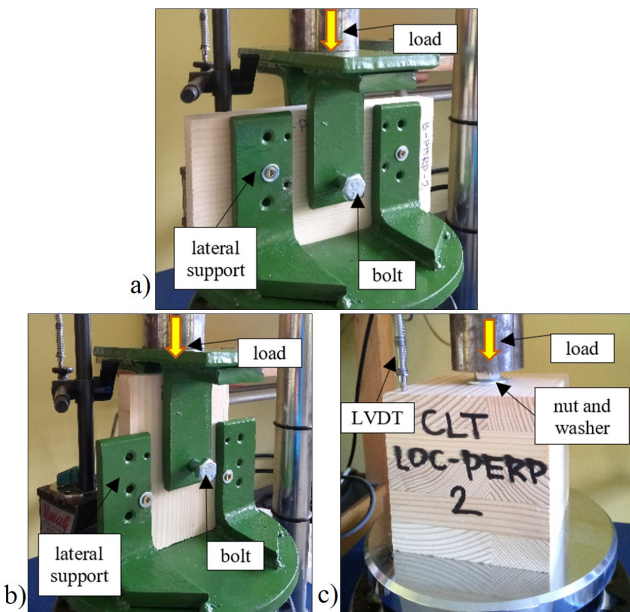


Fig. 5 (a), (b) Examination of timber under embedment pressure; (c) examination of the timber resistance at washer imprinting

defined. Behavior of timber under embedment pressure perpendicular (Fig. 5(a)) and parallel to the grain (Fig. 5(b)) has been examined on CLT panel specimens, according to the appropriate standard [33]. Moisture content in the specimens was 9.5%, and mass density was 420 kg/m³.

Examination of the timber resistance at washer imprinting into the CLT panel perpendicularly to the grain has been done on cube-shaped specimens with edge $a = 100$ mm, cut-out from the parts of the CLT panel undamaged after the push-out test (Fig. 5(c)).

Examination of the steel profile material and steel bolt material have been conducted using tension test on prepared coupons (Fig. 6(a) and (b)). Since the friction coefficient between steel profile and the CLT also affects the connection strength, it had been determined by appropriate testing before the push-out test, employing elements used for push-out test specimens (Fig. 6(c)). Three samples have been examined with three weights each (7.2 kg, 11.1 kg, and 19.4 kg), so that 9 results have been obtained in total.

The approx. values of obtained pressures in the sliding plane were: 0.40 N/cm², 0.60 N/cm², and 1.1 N/cm², respectively. All results from testing of timber, steel, and friction coefficient are presented in Section 3, along with adoption of adequate material models for numerical analysis.

3 Numerical model

The considered connection between the steel profile and the CLT panel has been modelled in full concordance with the specimens from the push-out test. Since the specimens have one plane of symmetry, only half of the specimen has been modelled, thus reducing the complexity of the model and solution time. Modelling, analysis, and post processing of the results has been done using the Finite element method and software Femap with NX Nastran [34]. Details of modelling are presented in the following text.

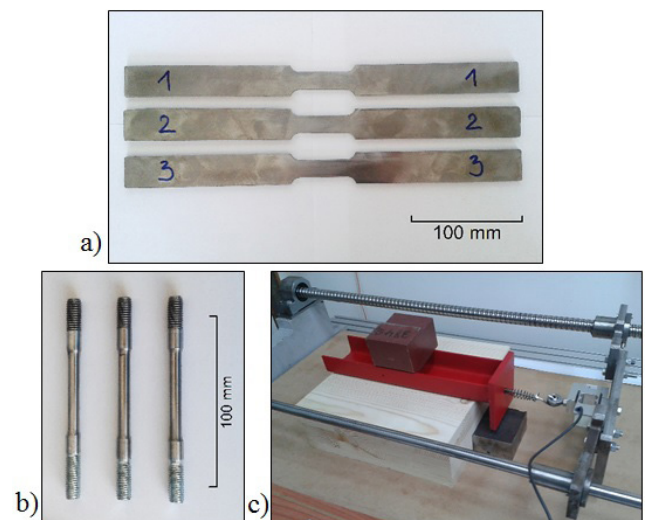


Fig. 6 Specimens: (a) steel S275 for tensile test, (b) steel 8.8 for tensile test, (c) steel profile-CLT panel for friction test

3.1 Modelling of the elements in the connection

The type of applied FE for a particular modelling component of the connection depended on the shape, material model and the role of the component in the connection, see Table 1.

3.1.1 Modelling of the steel profile and the bolt

Modelling of the steel profile included only the web being in contact with the timber material, and its dimensions were $\neq 100 \times 50 \times 4$ mm. Influence of the profile flange was replaced by rigid FE, using 2-node ROD FE (rigid rods 1, Fig. 7). Their stiffness was taken as $EA = 10^9$ N, and their length was $l = 100$ mm. The introduced rigid elements provide equal displacements of the connected nodes in X-direction, thus preventing steel web buckling.

Table 1 Modelling components, FE types, and appropriate material models

No.	Modelling component/function	FE type	Material model
1	Bolt	8-node SOLID	Multilinear plastic
2	Steel profile web	8-node SOLID	Multilinear plastic or linear elastic
3	Timber material around the bolt hole (parallel to the grain)	2-node ROD	Multilinear plastic
4	Timber material around the bolt hole (perpendicular to the grain)	2-node ROD	Multilinear plastic
5	Contact plate 1, 2, 3 (elements for contact forming)	4-node PLATE	Linear elastic
6	Interaction between bolt, nut, washer and timber surface	2-node ROD	Multilinear plastic
7	Auxiliary rigid rods 1, 2, 3	2-node ROD	Linear elastic (high stiffness)

The bolt shaft, head, and nut were modelled as a whole. The bolt shaft had dimensions $\text{Ø}10 \times 108$ mm, the head and the nut $\text{Ø}16 \times 7$ mm both, and the total length of the bolt was 122 mm.

Material models for the steel profile and for the bolt have been adopted based on the results of experimental testing (Table 2, Fig. 8). Nonlinear behavior of the steel profile web was expected only in the zone around the bolt hole spreading approximately $3d$ (d - bolt diameter) [3]. Consequently, the FE for the steel web have been defined as nonlinear only in the zone around the bolt hole 25 mm wide and 50 mm high, using elastoplastic multilinear material model. The remained elements have been set as linear-elastic. All elements of the bolt have been modelled as nonlinear using elastoplastic multilinear model.

3.1.2 Modelling of the timber parts of the CLT panel

Load transfer from the CLT panel to the bolt has been modelled with "timber rod" elements and "contact plate 1" elements, which formed the bolt hole. "Timber rod" elements were oriented in the direction of load acting (Z-direction), and their characteristics corresponded to the characteristics of timber regarding embedment pressure. Since the analyzed CLT panel consisted of five crisscrossed layers, it has been modelled in such a way that three groups of

Table 2 Steel material data

Part	Steel grade	Elasticity modulus [GPa]	Yield point [MPa]	Ultimate strength [MPa]
Steel profile	S275	200	330	460
Bolt	8.8	200	760	850

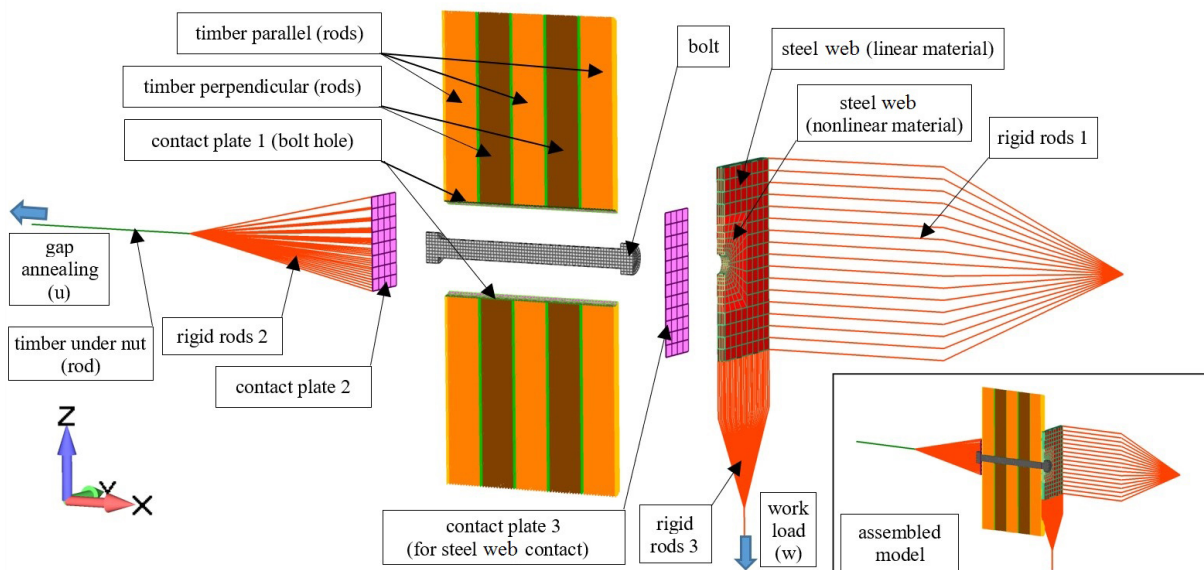


Fig. 7 An exploded view of the connection model, and the assembled connection model (bottom right)

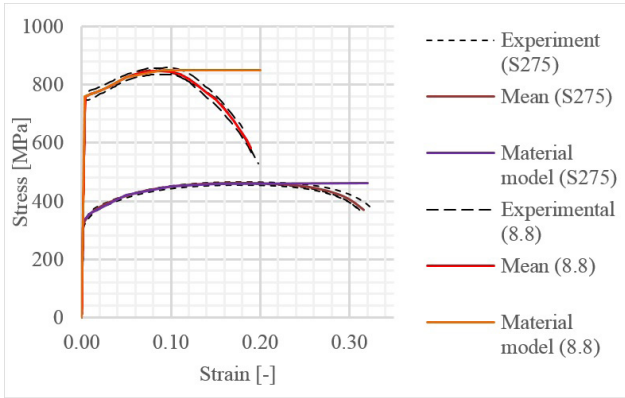


Fig. 8 Experimental stress-strain diagrams for steel material of the profile (S275) and the bolt (8.8)

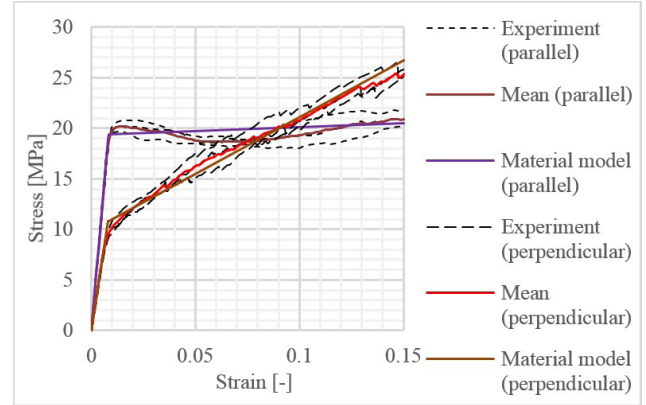


Fig. 9 Diagrams of the embedment pressure: experimental data and bilinear material law

elements had timber characteristics with grain parallel to the load direction, and two groups had timber characteristics with grain perpendicular to the load direction, in concordance with the layer setting. Cross-section area of the "timber rod" elements corresponded to the area in contact with the bolt shaft.

Stress-strain curves of the timber material loaded parallelly and perpendicularly to the grain (Fig. 9) have been determined using embedment test pressure (Fig. 5(a), (b)). This test gave corresponding forces and displacements transformed into average contact stress and strain by relations:

$$\sigma = F / (bd), \tag{1}$$

$$\varepsilon = c / l, \tag{2}$$

where:

- σ is embedment pressure,
- F is measured force value,
- b is specimen thickness ($b = 20$ mm),
- d is the bolt shaft diameter ($d = 10$ mm),
- ε is strain of timber rod element,
- c is measured displacement value,
- l is adopted length of the timber rod element ($l = 100$ mm).

For application in the numerical model, behavior of timber has been approximated by bilinear law, and the corresponding data are presented in Table 3 and Fig. 9.

Contact between the bolt shaft and the "timber rod" elements has been realized via "contact plate 1" elements (Fig. 10). They represented cylindrical surfaces around the bolt shaft, covering 54° of the central angle of the bolt shaft, both on the upper and bottom side. That way, they

Table 3 Timber rods - material data

Grain orientation	Elasticity modulus E [GPa]	Yield stress f_y [MPa]	Tangent modulus E_t [GPa]	Ratio E_t/E
Parallel	2.37	18.93	0.0079	0.0033
Perpendicular	1.35	10.79	0.112	0.0830

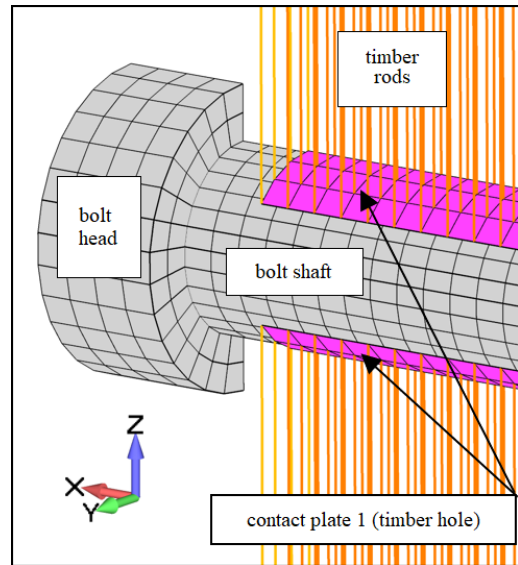


Fig. 10 Bolt and bolt hole – modelling detail

covered 60% of the bolt shaft perimeter. The remained part of the bolt shaft was uncovered because of the steep angle of the contact elements related to the shaft surface, and thus being inefficient for contact transfer. In order to minimize influence of their stiffness on the behavior of the connection, their thickness has been set to 0.1 mm, and their modulus of elasticity to $E = 0.001$ GPa. Mesh density of the "contact plate 1" elements was dictated by the mutual distances of the "timber rod" elements they were attached for.

3.1.3 Modelling of the system nut-washer-CLT panel

Interaction between the bolt, nut, washer, and the CLT panel has been modelled with element "timber under nut", (2-node ROD FE). Length of this element was $l = 100$ mm, and the cross-section area was equal to the pressure area of the washer onto the CLT panel ($A = 620$ mm²). Based on experimental data regarding forces and displacements, the curves of the timber behavior at local pressure perpendicular to the grain have been determined (Fig. 11). Experimental values of forces and displacements have been transformed into average contact stress and strain by the procedure analogous to the Eq. (1) and Eq. (2). In the numerical model, this behavior has been approximated by multilinear law. Obtained characteristics of the "timber under nut" element are given in Table 4.

One end of the "timber under nut" element was pin supported, and the other one was connected to the group of "rigid rod 2" elements. They connected "timber under nut" element with the "contact plate 2". The "contact plate 2" could move in X-direction only, and it made contact with the nut. Such disposition of elements enabled that the nut could move in X- and Z-direction, depending on the failure mode of the connection.

Before applying the work load, an initial moving of the "timber rod" element has been done, and it simulated tightening of the nut in order to anneal the gap between the connection parts. Gaps in the connection existed in

the model between the bolt head and the steel profile web, between the web and the "contact plate 3", and between the nut and the "contact plate 2". All three gaps have been set to 0.1 mm, and their annealing was accomplished by initial moving of the "timber under nut" element in negative X-direction for a value $u = 3 \times 0.1 = 0.3$ mm. Such modelling approach also enabled pretensioning of the bolt by initial moving of the "timber under nut" element for a value greater than 0.3 mm.

3.2 Modelling of contacts

For the detailed description of the behavior of the analyzed connection, the following "surface-to-surface" contacts have been modelled:

- between the bolt shaft (target) and the bolt hole in the CLT panel (contact plate 1, source),
- between the bolt shaft (target) and the bolt hole in the steel profile (source),
- between the steel profile web (source) and the CLT panel (contact plate 3, target),
- between the bolt head (source) and the steel profile web (target),
- between the nut (source) and the contact plate 2 (target).

Coulomb's friction has been included in all contacts, with a value $\mu = 0.35$ for contact between the steel profile and the CLT panel (determined experimentally), and $\mu = 0.20$ for the remained contacts, according to [35, 36].

3.3 Loading, boundary conditions, and analysis procedure

After the annealing of the gap described in Section 3.1.3, the connection was loaded applying the displacement $w = 16$ mm in negative Z-direction. Applying was done via the system of "rigid rod 3" elements (Fig. 7), which enabled equal displacements of all nodes of the bottom base of the steel web in Z-direction. Boundary conditions applied on the proposed connection model are presented in Fig. 12. All boundary conditions have been defined on nodes.

Models have been analyzed using the nonlinear analysis SOL601 (Advanced Nonlinear Analysis). Loads have been applied in 200 increments, with increment size 0.01. Fig. 13 presents the diagram of the load factors during the course of analysis.

3.4 Verification and validation of the FE model

Mesh sensitivity has been checked using coarse, medium, and fine FE mesh. Thereat, size of the FE elements of the

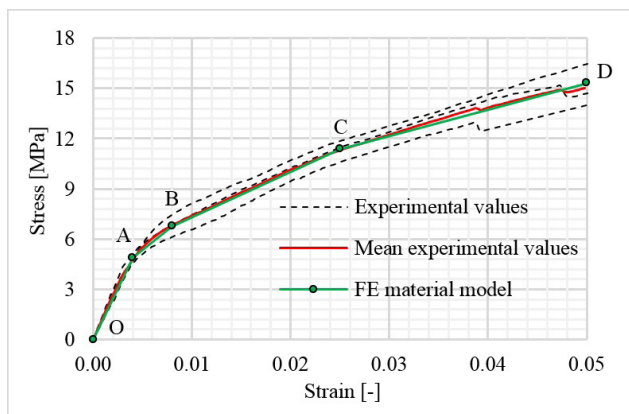


Fig. 11 Stress-strain curves for "timber under nut" element

Table 4 Timber rods - material data

Line segment (Fig. 11)	Stress at segment starting point [MPa]	Elasticity/tangent modulus E [GPa]	Ratio E_i/E
OA	0.00	1.23	-
AB	4.92	0.464	0.377
BC	6.77	0.270	0.220
CD	11.37	0.158	0.128

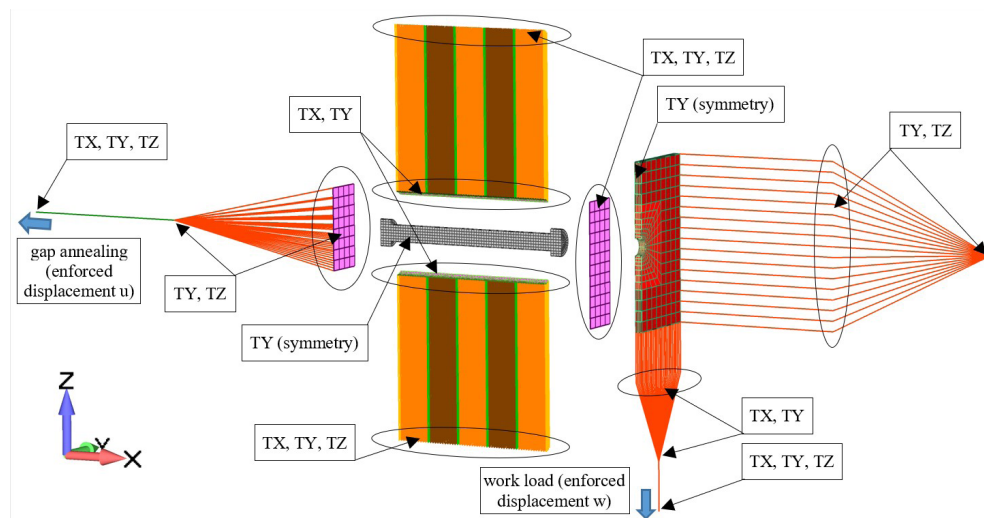


Fig. 12 Loading and boundary conditions (TX, TY, TZ – restrained displacements)

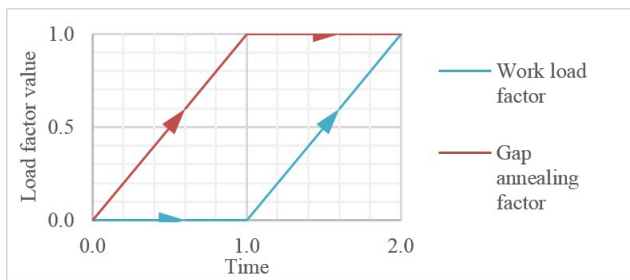


Fig. 13 Load factor diagrams

bolt was 2.5, 2.0, and 1.67 mm, respectively, and size of the FE elements of the steel profile web was 1.33, 1.0, and 0.8 mm (Fig. 14).

Diagrams in Fig. 15 represent experimental results (5 tests and mean values) and numerical results for three different mesh densities (coarse, medium and fine). It has to be remarked that the experimental analysis diagrams were shifted for clarity.

It can be seen from the diagrams that the results for three FE meshes coincide mutually, showing that the FE model was successfully verified. The numerical results agree well with the mean experimental results, serving as good validation of the FE model (Fig. 16). Based on the model verification, the medium mesh has been adopted for further analysis because it gave satisfying results and did not require high computer resources.

Table 5 presents comparative values of the connection characteristics obtained by experimental and numerical analysis. Thereat, strength represents the force in the connection registered at slip value of 15 mm, slip modulus represents the stiffness of the connection between 10% and 40% of strength, determined according to standard [32], and tangent slip modulus represents the stiffness

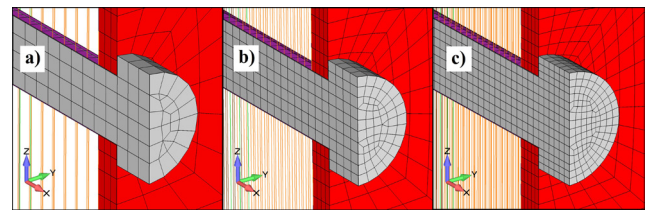


Fig. 14 Mesh density; (a) coarse, (b) medium, (c) fine

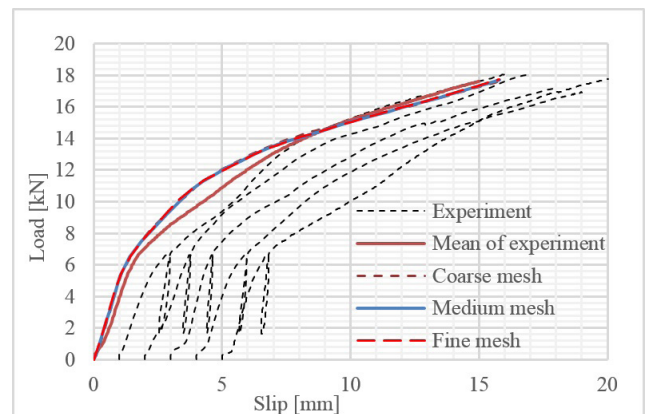


Fig. 15 Results of the numerical analysis for different FE mesh densities and results of the experimental analysis

Table 5 Comparison of the experimental and numerical results

Analysis method	Connection strength [kN]	Slip modulus [kN/mm]	Tangent slip modulus [kN/mm]
Experiment	17.6	3.69	0.426
FEM (medium mesh)	17.7	3.87	0.471
Δ (%)	0.1 (+1 %)	0.18 (+5 %)	0.045 (+11 %)

of the connection at slip value of 15 mm. Obtained value of the slip modulus is significant because it directly defines the stiffness of the composite connection.

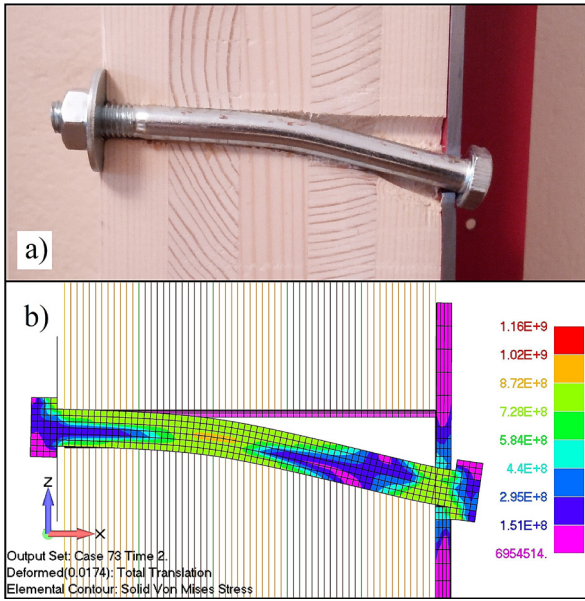


Fig. 16 Model validation – failure mode; (a) experiment; (b) numerical analysis (bolt von Mises stresses and deformation)

4 Parametric study

In order to investigate influence of different parameters of the connection on its behavior, a parametric study has been conducted, using the developed numerical model.

Thereat, the following parameters have been varied:

- bolt grade,
- bolt pretension force,
- thickness of the steel profile web.

Results of the parametric study are presented in the following text, and appropriate conclusions have been drawn.

4.1 Influence of bolt strength

For this study, five different grades of steel have been employed for bolt material, and their characteristics are presented in Fig. 17. The stress-strain curves for steel grade 4.6, 8.8, and 12.9 have been adopted according to literature data [5, 37]. The bolt with grade 8.8 has been also examined experimentally, and since its stress-strain curve differed from those taken from literature, it was taken as a separate case.

Table 6 presents values of the connection strength, slip modulus, and tangent slip modulus. The case for the bolt grade 8.8 with tested characteristics was adopted as reference, and the deviations of output values of all other cases are given in brackets.

Analysis results regarding the connection strength and tangent slip modulus were as expected, meaning that application of bolts with higher strength gave higher

connection strength. On the other hand, the stiffness modulus decreased with the increase of the bolt grade. Reason for this was the applied calculation method, taken from the standard [32]. Application of the bolt with grade 8.8, whether for the nominal or for the tested input data, exhibited mutually very close values of the connection characteristics (Fig. 18).

Different bolt strengths produced failure modes with two, one or none plastic hinges. In this study, particular interest draws the case with bolt grade 4.6 and two plastic hinges (Fig. 19(a)). According to Eurocode 5 [38], the case with ratio of the steel plate thickness and bolt diameter $t/d \leq 0.5$ implies that failure modes without plastic hinges (Fig. 19(c)) or with one plastic hinge (Fig. 19(b)) are only possible. Reason for this is the opinion that thin steel plate cannot generate fixing moment needed for occurrence of the plastic hinge in the slipping plane, near the bolt head. This moment arises in two ways. The first one is fixing of the bolt shaft into the steel plate. For generating of the

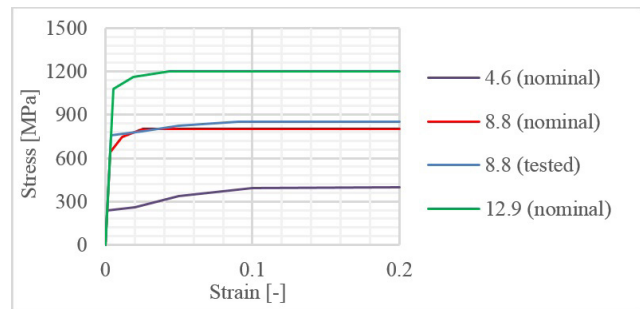


Fig. 17 Stress-strain curves for different grades of bolt material

Table 6 Influence of bolt strength on connection characteristics

Bolt grade	Connection strength [kN]	Slip modulus [kN/mm]	Tangent slip modulus [kN/mm]
4.6 (nominal)	12.2 (-31 %)	5.05 (+30 %)	0.420 (-11 %)
8.8 (nominal)	17.3 (-2 %)	3.91 (+1 %)	0.453 (-4 %)
8.8 (tested, reference)	17.7	3.87	0.471

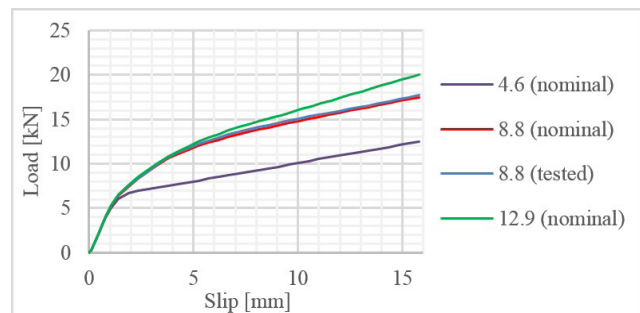


Fig. 18 Load-slip curves for different grades of bolt material

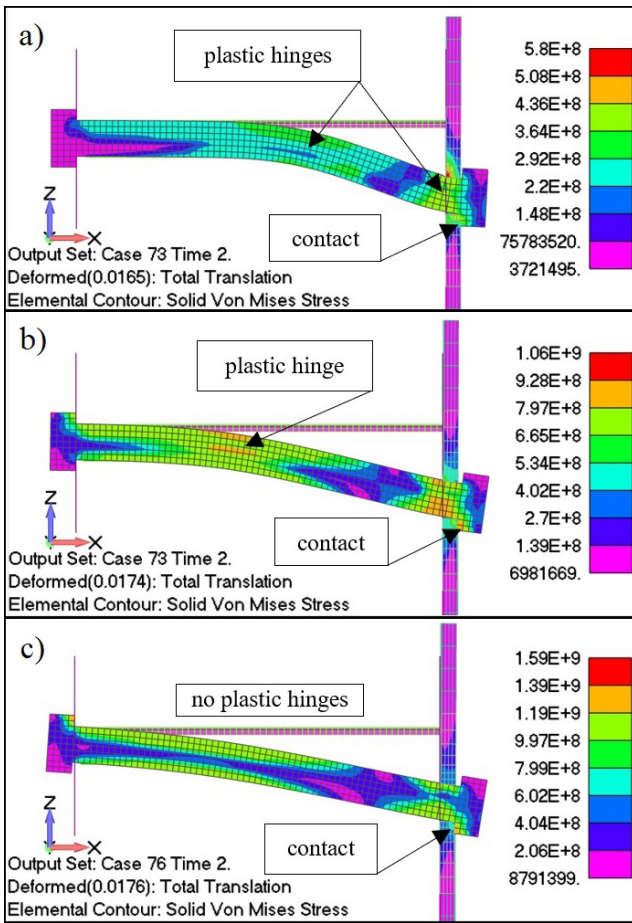


Fig. 19 Failure modes for different bolt grades; deformation and von Mises stress contours: a) 4.6, b) 8.8, c) 12.9

moment, it is necessary for the plate to be thick enough ($t/d \geq 1.0$), which Eurocode prescribes, too. The second way of moment generating arises as the consequence of introducing of an axial force into the bolt due to its withdrawal resistance. The inclination of the bolt head affects that the axial force is introduced via the bottom edge of the bolt head, and not through its whole perimeter. Therefore, a moment equal to the product of the bolt axial force and the head radius arises. That moment exists in all cases where the withdrawal resistance exists (Fig. 19(a)–(c)). In case of a bolt with grade 4.6 (Fig. 19(a)), that moment has enough intensity to generate a plastic hinge, while in other cases its intensity is not enough to generate a plastic hinge.

4.2 Influence of bolt pretensioning

Pretension of the bolt can be introduced into the connection model by moving the support of the "timber under nut" element for a value greater than the total gap value of 0.3 mm in the connection (Section 3.1.3). In this research, three different bolt pretension forces, that is, three different

support displacements have been applied: 1.0, 2.0, and 3.0 mm. All these displacements were added to the initial value of 0.3 mm. Dependences load vs. slip and bolt axial force vs. slip are presented in Fig. 20 and Fig. 21, respectively, for different values of the pretension.

Table 7 presents values of the characteristic output values of the connection as a function of bolt pretension. The parametric case without pretension was adopted as reference, and the deviations of output values of all other cases are given in brackets.

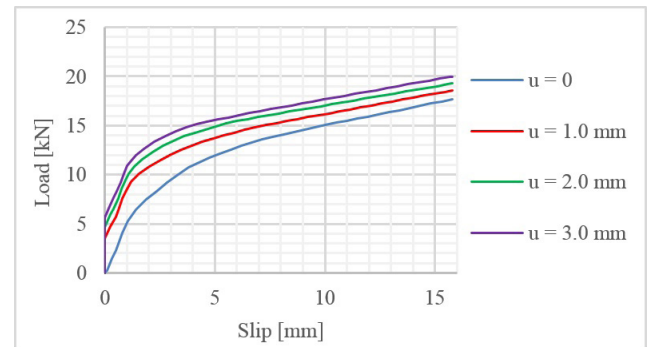


Fig. 20 Load-slip diagram of the connection depending on the bolt-pretension

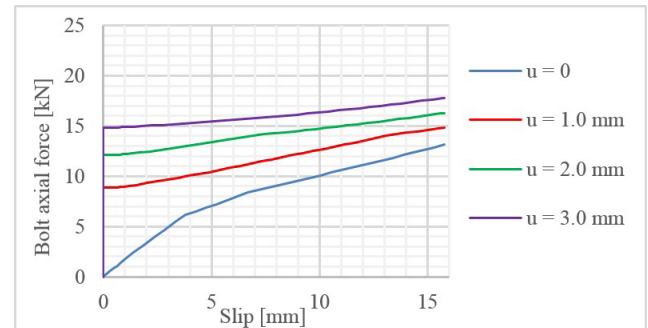


Fig. 21 Bolt axial force-slip diagram depending on the bolt-pretension

Table 7 Influence of bolt strength on connection characteristics

Support displacement u [mm]	0.0 (ref.)	1.0	2.0	3.0
Bolt pretensioning force [kN]	0.1	8.8	12.1	14.9
Max. connection force (no slip) [kN]	0.0	3.4	4.6	5.6
Bolt axial force (ultimate) [kN]	12.8	14.7 (+15 %)	16.0 (+25 %)	17.6 (+38 %)
Connection strength [kN]	17.7	18.4 (+4 %)	18.9 (+7 %)	19.7 (+11 %)
Slip modulus [kN/mm]	3.87	7.23 (+87 %)	9.52 (+146 %)	15.32 (+296 %)
Tangent slip modulus [kN/mm]	0.471	0.392 (-17 %)	0.391 (-17 %)	0.398 (-15 %)

The results show that, with increase of the bolt pretensioning, strength and stiffness of the connection also increased, as expected. The bolt pretensioning force generated an initial axial force in the bolt shaft, and consequently, a friction force in the slipping plane occurred. This friction prevented slipping in the connection until the work load surpassed the intensity of the friction force. This caused major increase of the connection stiffness, but minor increase the connection strength.

4.3 Influence of the steel profile web thickness

Ratio between the steel profile web thickness and the bolt diameter (t/d) is an important factor, because it affects the failure mode of the connection. In this research, only the thickness of the steel profile web has been varied, while the bolt diameter has been kept constant. According to Eurocode 5 [38], the connection between the profile web and the bolt is considered as pinned if $t/d \leq 0.5$, and as fixed if $t/d \geq 1.0$. Between these values, it is considered as semi-rigid. In the experimental part of this research, this ratio was $t/d = 0.4$, so it can be assumed that the connection was pinned. In the numerical model, three different thicknesses of the steel profile have been analyzed, and the load-slip and the bolt axial force-slip diagrams are presented in Figs. 22 and 23.

Table 8 presents values of the characteristic output values of the connection as a function of the steel profile web thickness. The case with steel profile web thickness $t = 4$ mm was adopted as reference, and the deviations of output values of all other cases are given in brackets.

It has been expected that higher thickness of the steel profile web would give higher connection strength, but that was not the case in this research. The explanation lies in the phenomenon known as rope effect [39]. Namely, if the connection of the bolt and the steel profile is pinned, rotation of the bolt head generates higher axial force in the bolt than in case of thicker steel profile (Fig. 24), leading to higher connection strength.

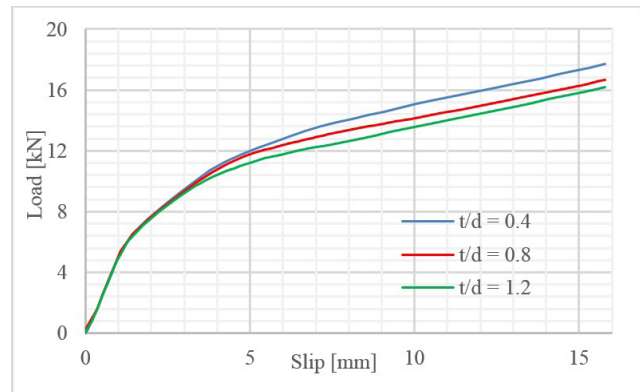


Fig. 22 Behavior of the connection as a function of the steel profile web thickness: load-slip curves

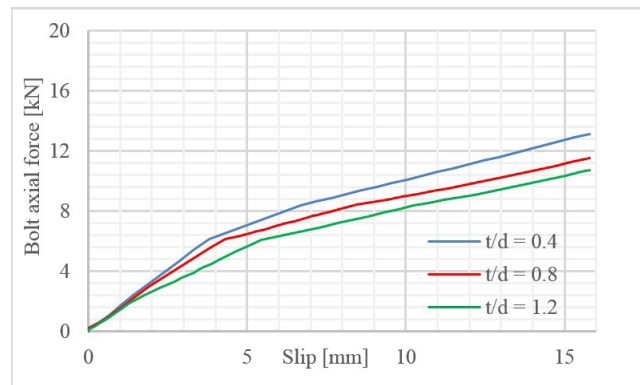


Fig. 23 Behavior of the connection as a function of the steel profile web thickness: bolt axial force-slip diagram

Table 8 Influence of the steel profile web thickness on connection characteristics

Steel web thickness [mm]	4 (reference)	8	12
Connection strength [kN]	17.7	16.4 (-7 %)	15.8 (-9 %)
Bolt axial force (ultimate) [kN]	12.8	11.1 (-13 %)	10.3 (-20 %)
Slip modulus [kN/mm]	3.87	4.77 (+23 %)	4.79 (+24 %)
Tangent slip modulus [kN/mm]	0.471	0.465 (-1 %)	0.474 (+1 %)

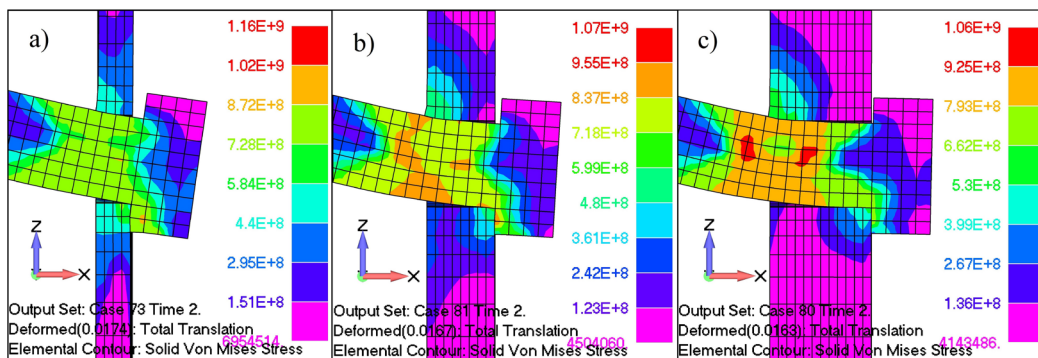


Fig. 24 Rotation of the bolt head for different steel web thicknesses; (a) $t = 4$ mm, (b) $t = 8$ mm, (c) $t = 12$ mm

As seen from the previous text and from the Fig. 24, rope effect may greatly affect the behavior of the connection. In order to confirm its influence, analyses with excluded rope effect have been conducted. For that purpose, the elements "timber under nut", "rigid rods 2" and "contact plate 2" have been omitted, and the friction between the bolt shaft and the bolt hole ("contact plate 1") was annealed. Results of this analysis are presented in Fig. 25, Fig. 26, and in Table 9. The case with steel profile web thickness $t = 4$ mm was adopted as reference, and the deviations of output values of all other cases are given in brackets.

Diagram in Fig. 25 presents load-slip dependence in the models without rope effect, which means that here only the primary (Johansen's) strength existed. In the case where $t = 4$ mm ($t/d = 0.4$, Fig. 26(a)), the bolt was not fixed into the profile web, so a relatively large rotation of the bolt head occurred, and there was one plastic hinge inside the CLT panel. In cases where thickness of the profile web was $d = 8$ mm ($t/d = 0.8$, Fig. 26(b)), and $d = 12$ mm ($t/d = 1.2$, Fig. 26(c)), the connection strength was approximately equal, which meant that fixing was already present when $d = 8$ mm. Significant difference between the cases $t/d = 0.8$ and $t/d = 1.2$ was reflected only in their slip moduli. It has been noted that in case where $t/d = 0.8$ it was necessary for the bolt head to perform larger rotation to achieve fixing. Eurocode 5 is conservative in this issue, because it states that in this case the connection of the bolt and the steel profile acts as semi-rigid.

5 Discussion

Specificity in the modelling process in this research was that in the proposed model ROD FE have been used for timber modelling, and PLATE FE with negligible stiffness as auxiliary elements for modelling the contact between the bolt and the timber.

The model is additionally simplified using symmetry, and thus modelling only half of the complete model. Regarding the input data for the timber material, only examination of timber on embedment pressure and on local pressure of the washer onto timber is needed.

Verification of the developed FE model had been conducted applying three mesh densities, with almost total agreement. Validation of the model has been conducted by experimental analysis. Experimental research was done using the asymmetrical (pure shear) push-out test with lateral supporting of the immovable part of the specimen. It was proved that this type of testing is reliable and rational. Namely, it requires half of the material needed

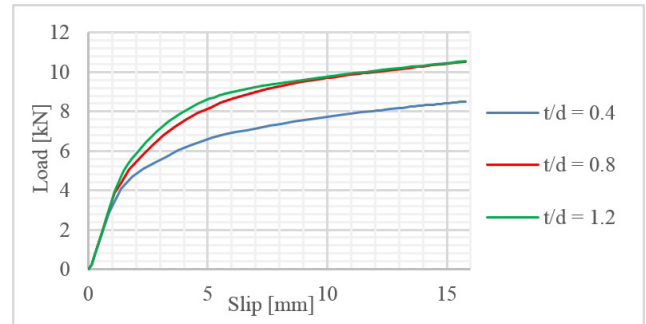


Fig. 25 Load-slip diagram without rope effect

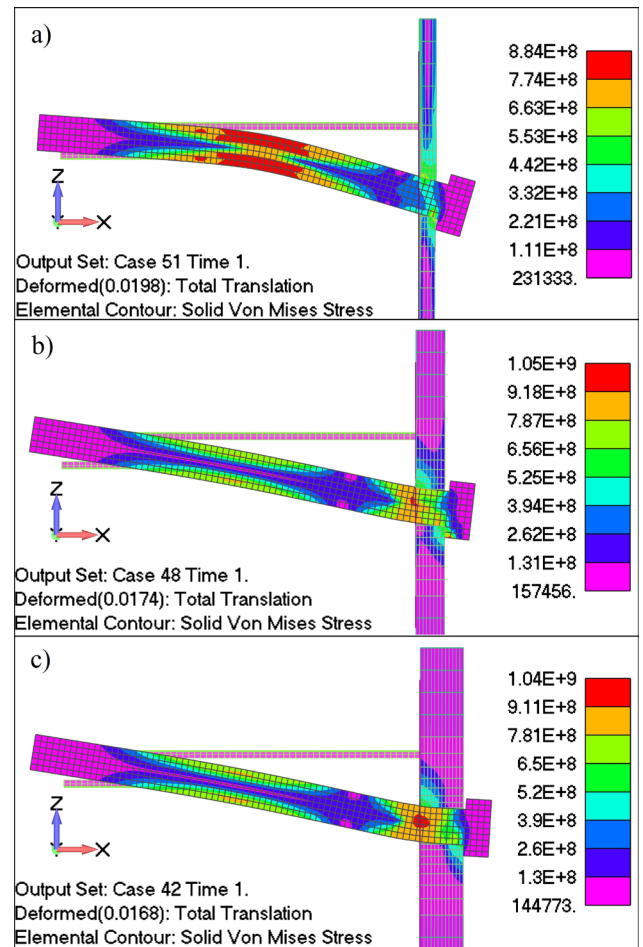


Fig. 26 Failure modes without rope effect: (a) $t = 4$ mm, (b) $t = 8$ mm, (c) $t = 12$ mm

Table 9 Influence of the steel profile web thickness on connection characteristics

Steel web thickness [mm]	4 (reference)	8	12
Connection strength [kN]	8.4	10.4 (+24 %)	10.5 (+25 %)
Slip modulus [kN/mm]	2.84	3.35 (+18 %)	3.82 (+35 %)
Tangent slip modulus [kN/mm]	0.115	0.134 (+17 %)	0.127 (+10 %)

for specimen production, lower load level, and less measuring instruments (two LVDT instead of four in symmetrical push-out test). The drawback of the asymmetrical test compared to the symmetrical is occurrence of the normal stress in the slipping plane. In the experimental testing within this research, this was prevented by reducing the load eccentricity to minimum. Using comparative analysis of the numerical and experimental results, it has been determined that the deviations regarding connection strength and stiffness are minimal. The failure modes were the same for both analyses, so all these facts confirmed the validity of the proposed model.

The proposed model has been used for parametric analysis, in order to examine the connection behavior in case of varying several parameters: bolt grade, bolt pretension force, and steel web thickness.

Variation of the bolt grade has different effects. Increase of the bolt grade increases the connection strength and the tangent slip modulus, while the slip modulus decreases.

The connection with the bolt grade 4.6 exhibits certain anomaly. According to EC 5, in case of thin steel profile web ($t/d \leq 0.5$) the connection between the bolt head and the web is considered as pinned. In this research, the steel web fulfilled the condition for a thin one ($t/d = 0.4$), but the numerical results showed that the connection acted as fixed.

Bolt pretensioning increases the axial force in the bolt, and consequently increases the strength of the connection to the certain degree, but far more its stiffness.

Varying of the thickness of the steel profile web also shows irregularities in behavior. The EC 5 implies that connection strength is higher or remains constant if the steel profile web is increased. However, in this research, higher thickness of the steel profile web increased the connection stiffness significantly, but due to the less prominent rope effect, the connection strength decreased.

Further improvements in the methodology of calculation of this type of connection would imply generating of a reliable database which contents the characteristics of the timber material that are necessary for application of the proposed FE model, thereby the demanding experimental tests would be avoided.

6 Conclusions

In the paper has been proposed an innovative numerical model of bolted composite connection between steel profile and 5-layer CLT panel. The innovativity is reflected in the introduction of a new approach for hybrid modeling of the CLT panel. The proposed numerical model is

simple for application because the applied material models are already defined in available engineering software for nonlinear analysis.

Using the proposed model, a parametric study that included varying of the bolt grade, pretension level, and web profile thickness, has been conducted. Taking an insight into the results, one may conclude that low bolt grades give low strength and high stiffness, and vice versa. Although the strength and stiffness of the composite structure is significantly affected by the strength and stiffness of the shear connectors, increase of the bolt grade may not lead to the higher bearing capacity of the composite structure. Consequently, extremely high or extremely low bolt grades are not recommended.

Using of low-grade bolts, an anomaly expressed as failure with two plastic hinges in the bolt occurred, which is not defined in the EC5. This alteration in behavior is a consequence of the rope effect, which generates axial force in the bolt shaft, tightens the bolt head to the steel profile web and prevents rotation needed for pinned connection. This phenomenon is manifested only for specific ratios of the bolt withdrawal strength and the bolt yield moment.

In case of varying of pretension, increase of stiffness is caused by high amount of the friction force in the slipping plane generated by pretensioning force. In the practical sense, pretensioning reduces the slipping and makes the composite connection closer to the rigid–ideal plastic behavior that is the most favorable for composite structures.

Varying of the steel web thickness also gave unexpected results: higher web thickness produced lower connection strength. Reason for this is because higher web thickness generates lower axial force in the bolt, and thereby lower connection strength. The influence of the rope effect on connection strength was additionally confirmed on the FE models that lack the nut and the washer, thus being unable to generate axial force in the bolt. Analysis showed that absence of the rope effect produced results that correspond to the EC 5 postulates.

The phenomenon of the rope effect in bolted composite connections has not been thoroughly considered in the up-to-date research. It has been showed in this paper that its influence provides significant benefits for this type of connection. Its contribution to the connection strength was confirmed by parametric study of the influence of the bolt grade, pretensioning force, and steel web thickness.

The calculation procedure of the examined connection given in EC 5 is oversimplified because the primary (Johansen) and the secondary (rope effect) strength are

considered as independent values that are summed up at the end. On the other hand, an analytical calculation method that would integrally consider the primary and secondary strength component would be far too complex. The proposed numerical model encompasses the rope effect phenomenon completely, and also includes influences of additional parameters, like bolt grade, pre-tensioning force, and steel profile web thickness, which may be easily varied in design practice.

References

- [1] Hong, J.-P., Kim, H.-B., Oh, J.-K., Lee, J.-J. "Dowel-embedment Properties-Based Finite Solid Element Model for Bolted Connections", *Journal of the Korean Wood Science and Technology*, 42(5), pp. 563–570, 2014.
<https://doi.org/10.5658/WOOD.2014.42.5.563>
- [2] Sandhaas, C. "Mechanical behaviour of timber joints with slotted-in steel plates", PhD Thesis, Delft University of Technology, 2012.
- [3] Gharib, M., Hassanieh, A., Valipour, H., Bradford, M. A. "Three-dimensional constitutive modelling of arbitrarily orientated timber based on continuum damage mechanics", *Finite Elements in Analysis and Design*, 135, pp. 79–90, 2017.
<https://doi.org/10.1016/j.finel.2017.07.008>
- [4] Sandhaas, C., Sarnaghi, A. K., van de Kuilen, J.-W. "Numerical modelling of timber and timber joints: computational aspects", *Wood Science and Technology*, 54(1), pp. 31–61, 2020.
<https://doi.org/10.1007/s00226-019-01142-8>
- [5] Hassanieh, A., Valipour, H. R., Bradford, M. A. Sandhaas, C. "Modelling of steel-timber composite connections: Validation of finite element model and parametric study", *Engineering Structures*, 138, pp. 35–49, 2017.
<https://doi.org/10.1016/j.engstruct.2017.02.016>
- [6] Akter, S. T., Serrano, E., Bader, T. K. "Numerical modelling of wood under combined loading of compression perpendicular to the grain and rolling shear", *Engineering Structures*, 244, 112800, 2021.
<https://doi.org/10.1016/j.engstruct.2021.112800>
- [7] Saad, K., Lengyel, A. "Inverse Calculation of Timber-CFRP Composite Beams Using Finite Element Analysis", *Periodica Polytechnica Civil Engineering*, 65(2), pp. 437–449, 2021.
<https://doi.org/10.3311/PPci.16527>
- [8] Saad, K., Lengyel, A. "A Parametric Investigation of the Influence of Knots on the Flexural Behavior of Timber Beams", *Periodica Polytechnica Civil Engineering*, 67(1), pp. 261–271, 2023.
<https://doi.org/10.3311/PPci.21360>
- [9] Wittel, F. K., Dill-Langer, G., Kröplin, B.-H. "Modeling of damage evolution in soft-wood perpendicular to grain by means of a discrete element approach", *Computational Materials Science*, 32(3–4), pp. 594–603, 2005.
<https://doi.org/10.1016/j.commatsci.2004.09.004>
- [10] Reichert, T. "Development of 3D Lattice Models for Predicting Non-linear Timber Joint Behaviour", PhD Thesis, Edinburgh Napier University, 2009.
- [11] Milić, M., Petronijević, P., Vacev, T., Zorić, A., Nešović, I. "Design of Nailed Timber-Concrete Composite Joint according to Eurocode and FEA", *Facta Universitatis, Series: Architecture and Civil Engineering*, 20(3), pp. 301–311, 2022.
<https://doi.org/10.2298/FUACE221112022M>
- [12] Racher, P., Bocquet, J. F. "Non-linear analysis of dowelled timber connections: a new approach for embedding modelling", *Electronic Journal of Structural Engineering*, 5, pp. 1–9, 2005.
<https://doi.org/10.56748/ejse.546>
- [13] Toussaint, P. "Application et modélisation du principe de la précontrainte sur des assemblages de structure bois" (Application and modeling of the principle of prestressing on wooden structure assemblies), PhD Thesis, Université Henri Poincaré, 2010. (in French)
- [14] Tavakoli-Gheynani, I. "Modélisation tridimensionnelle d'assemblages de structure bois en tôle pliée mince par la méthode des éléments finis" (Three-dimensional modeling of wooden structure assemblies in thin bent sheet metal by the finite element method), PhD Thesis, Université Henri Poincaré, 2011. (in French)
- [15] Chiniforush, A. A., Valipour, H. R., Bradford, M. A., Akbarnezhad, A. "Long-term behaviour of steel-timber composite (STC) shear connections", *Engineering Structures*, 196, 109356, 2019.
<https://doi.org/10.1016/j.engstruct.2019.109356>
- [16] Schiro, G., Giongo, I., Sebastian, W., Riccadonna, D., Piazza, M. "Testing of timber-to-timber screw-connections in hybrid configurations", *Construction and Building Materials*, 171, pp. 170–186, 2018.
<https://doi.org/10.1016/j.conbuildmat.2018.03.078>
- [17] Hassanieh, A., Valipour, H. R., Bradford, M. A. "Load-slip behaviour of steel-cross laminated timber (CLT) composite connections", *Journal of Constructional Steel Research*, 122, pp. 110–121, 2016.
<https://doi.org/10.1016/j.jcsr.2016.03.008>
- [18] Yang, R., Li, H., Lorenzo, R., Ashraf, M., Sun, Y., Yuan, Q. "Mechanical behaviour of steel timber composite shear connections", *Construction and Building Materials*, 258, 119605, 2020.
<https://doi.org/10.1016/j.conbuildmat.2020.119605>
- [19] Vella, N., Gardner, L., Buhagiar, S. "Experimental analysis of cold-formed steel-to-timber connections with inclined screws", *Structures*, 24, pp. 890–904, 2020.
<https://doi.org/10.1016/j.istruc.2020.02.009>
- [20] Erdélyi, S., Dunai, L. "Behaviour of a New Type of Composite Connection", *Periodica Polytechnica Civil Engineering*, 48(1–2), pp. 89–100, 2004. [online] Available at: <https://pp.bme.hu/ci/article/view/585/0>

Acknowledgements

The authors express their gratitude to the Ministry of Education, Science and Technological Development of the Republic of Serbia for partial support in this research. They would also like to thank to the Laboratory for Geotechnics of the Faculty of Civil Engineering and Architecture in Niš, Serbia, the Laboratory for Materials and Machine Testing and the Laboratory for Machine Design of the Faculty of Mechanical Engineering in Niš, Serbia, and to the "Kolarević Company" in Čičevac, Serbia.

- [21] Aicher, S., Hirsch, M., Christian, Z. "Hybrid cross-laminated timber plates with beech wood cross-layers", *Construction and Building Materials*, 124, pp. 1007–1018, 2016.
<https://doi.org/10.1016/j.conbuildmat.2016.08.051>
- [22] Cao, J., Xiong, H., Wang, Z., Chen, J. "Experimental investigation and numerical analysis for concrete-CLT connections", *Construction and Building Materials*, 236, 117533, 2020.
<https://doi.org/10.1016/j.conbuildmat.2019.117533>
- [23] Lukaszewska, E., Johnsson, H., Fragiaco, M. "Performance of connections for prefabricated timber–concrete composite floors", *Materials and Structures*, 41(9), pp. 1533–1550, 2008.
<https://doi.org/10.1617/s11527-007-9346-6>
- [24] Crocetti, R., Sartori, T., Tomasi, R. "Innovative timber-concrete composite structures with prefabricated FRC slabs", *Journal of Structural Engineering*, 141(9), 04014224, 2015.
[https://doi.org/10.1061/\(ASCE\)ST.1943-541X.0001203](https://doi.org/10.1061/(ASCE)ST.1943-541X.0001203)
- [25] Deam, B. L., Fragiaco, M., Buchanan, A. H. "Connections for composite concrete slab and LVL flooring systems", *Materials and Structures*, 41(3), pp. 495–507, 2008.
<https://doi.org/10.1617/s11527-007-9261-x>
- [26] Djoubissie, D. D., Messan, A., Fournely, E., Bouchaïr, A. "Experimental study of the mechanical behavior of timber-concrete shear connections with threaded reinforcing bars", *Engineering Structures*, 172, pp. 997–1010, 2018.
<https://doi.org/10.1016/j.engstruct.2018.06.084>
- [27] Khorsandnia, N., Valipour, H. R., Keith, C. "Experimental and analytical investigation of short-term behaviour of LVL–concrete composite connections and beams", *Construction and Building Materials*, 37, pp. 229–238, 2012.
<https://doi.org/10.1016/j.conbuildmat.2012.07.022>
- [28] Tonon, J. E., Moreno, J. R. S., Francisco, J. C. S., Fogal, M. L. F. "Evaluation of shear resistance of bolted connections in wood/wood and wood/steel plate/wood", *American Journal of Materials Science*, 5(2), pp. 47–52, 2015.
<https://doi.org/10.5923/j.materials.20150502.04>
- [29] Wang, C.-L., Lyu, J., Zhao, J., Yang, H. "Experimental investigation of the shear characteristics of steel-to-timber composite joints with inclined self-tapping screws", *Engineering Structures*, 215, 110683, 2020.
<https://doi.org/10.1016/j.engstruct.2020.110683>
- [30] CEN "BS EN 16351:2021 Timber structures. Cross laminated timber. Requirements", European Committee for Standardization, Brussels, Belgium, 2021.
- [31] CEN "EN 338 Structural timber - Strength classes", European Committee for Standardization, Brussels, Belgium, 2009.
- [32] CEN "BS EN 26891:1991 Timber Structures - Joints Made with Mechanical Fasteners - General Principles for the Determination of Strength and Deformation Characteristics", European Committee for Standardization, Brussels, Belgium, 1991.
- [33] CEN "EN 383:2007 Timber Structures - Test methods - Determination of embedment strength and foundation values for dowel type fasteners", European Committee for Standardization, Brussels, Belgium, 2007.
- [34] Siemens "FEMAP with NX NASTRAN: Software documentation", 2017. [online] Available at: https://www.dex.siemens.com/plm/femap/femap-with-nx-nastran?cclcl=en_US
- [35] CEN "EN 1993-2 Eurocode 3: Design of steel structures. Part 2: Steel Bridges", European Committee for Standardization, Brussels, Belgium, 2006.
- [36] Sayir, M., Dual, J., Kaufmann, S., Mazza, E. "Ingenieurmechanik 1: Grundlagen und Statik" (Engineering Mechanics 1: Basics and Statics), Springer Vieweg, Teubner Verlag Wiesbaden, 2015. (in German) ISBN: 978-3-8351-9244-7
<https://doi.org/10.1007/978-3-8351-9244-7>
- [37] Dessouki, A. K., Youssef, A. H., Ibrahim, M. M. "Behavior of I-beam bolted extended end-plate moment connections", *Ain Shams Engineering Journal*, 4(4), pp. 685–699, 2013.
<https://doi.org/10.1016/j.asej.2013.03.004>
- [38] CEN "EN 1995-1-1 Eurocode 5: Design of timber structures - Part 1-1: General - Common rules and rules for buildings", European Committee for Standardization, Brussels, Belgium, 2004.
- [39] Gečys, T., Bader, T. K., Olsson, A., Kajėnas, S. "Influence of the rope effect on the slip curve of laterally loaded, nailed and screwed timber-to-timber connections", *Construction and Building Materials*, 228, 116702, 2019.
<https://doi.org/10.1016/j.conbuildmat.2019.116702>